Synergistic Apoptosis

DOI: 10.1002/anie.201206400

Double-Effector Nanoparticles: A Synergistic Approach to Apoptotic Hyperthermia**

Dongwon Yoo, Heeyeong Jeong, Christian Preihs, Jin-sil Choi, Tae-Hyun Shin, Jonathan L. Sessler, and Jinwoo Cheon**

Temperature control is an important method of self-defense in biological systems. For example, one response mounted by humans in an effort to fight injury, including viral and bacterial infections, involves an increase in body temperature, thus producing the well-recognized symptoms of fever.[1] Today, the idea of using artificial temperature control for disease removal is being realized with the aid of various techniques, such as ultrasound, near-infrared light, and magnetic field by increasing localized temperature in a targeted region.[2] Magnetic nanoparticles have attracted considerable attention for hyperthermia applications owing to their ability to generate heat effectively when exposed to an alternating magnetic field without a penetration depth limit.[3] Hyperthermia, the artificially induced heat treatment of a disease, uses temperatures ranging between 42 °C and 47 °C. Generally, a temperature below 45 °C induces apoptotic cell death.[4] As compared to necrosis, apoptosis is a more benign form of "programmed" cell death.[5] Nonliving cells produced as the result of apoptotic process are cleaned by phagocytosis without affecting neighboring normal cells. In contrast, necrosis, typically generated by harsh and high-temperature hyperthermia, is considered relatively harmful because it can be correlated with inflammatory disease and metastasis.[6] However, achieving effective apoptotic hyperthermia is often difficult, as cells typically acquire resistance to induced thermal stress.[7] Repeated exposures to high temperatures with high concentration of magnetic nanoparticles are usually necessary to achieve a useful level of therapeutic efficacy even though the conditions could favor necrotic cell death rather than apoptosis. Because cancer cells are susceptible to heat at about 43 °C, while most normal tissues remain undamaged,[8] hyperthermia using this temperature defines a recognized but unmet goal.

[*] Dr. D. Yoo,[+] H. Jeong,[+] Dr. J.-s. Choi, T.-H. Shin, Prof. J. Cheon
Department of Chemistry, Yonsei University
Seoul 120-749 (Korea)
E-mail: jcheon@yonsei.ac.kr
C. Preihs, Prof. J. L. Sessler
Department of Chemistry and Biochemistry, University of Texas
1 University Station-A5300, Austin, TX 78712-0165 (USA)
E-mail: sessler@cm.utexas.edu
[+] These authors contributed equally to this work.

[**] This work was financially supported by grants from the Creative Research Initiative (2010-0018286), WCU Program (R32-2009-10217), and BK21 for Chemistry. The work in Austin was supported by the National Institutes of Health (grant CA 68682) and the Robert A. Welch Foundation (grant F-1018).
Supporting information for this article is available on the WWW under http://dx.doi.org/10.1002/anie.201206400.

In this study, we introduce a new design concept of double-effector magnetic nanoparticle system for high-performance apoptotic hyperthermia. Double-effector nanoparticles are composed of two functional components, which serve as sources of reactive oxygen species (ROS) and heat. We demonstrate that ROS-generating magnetic nanoparticles can effectively sensitize cancer cells to make them highly vulnerable to subsequent apoptotic magnetic hyperthermia at low temperatures (Scheme 1).

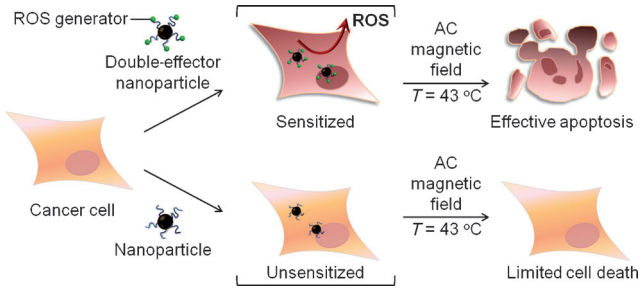

Scheme 1. Double-effector nanoparticles for effective apoptotic magnetic hyperthermia. The nanoparticles generate reactive oxygen species (ROS) to sensitize cancer cells for hyperthermia even under low-temperature conditions (ca. 43 °C). The sensitization strategy is effective for apoptotic hyperthermia both in vitro and in vivo, whereas conventional unsensitized hyperthermia shows marginal efficacy.

A gadolinium(III) texaphyrin is used as the ROS-producing sensitizer. Texaphyrins are pentaaza expanded porphyrins, and one particular gadolinium(III) texaphyrin, known as motexafin gadolinium (MGd), has been shown to generate ROS by depleting so-called reducing metabolites within cancer cells.[9] The magnetic nanoparticles are $Zn_{0.4}Fe_{2.6}O_4$, with a diameter of 15 nm, that possess highly efficient heat-generating capability under an AC magnetic field (core MNPs).[10]

A summary of the synthetic routes used to conjugate gadolinium(III) texaphyrins (GdTx) to core-MNPs is shown in Figure 1 a. Silica-coated core MNPs with polyethylene glycol (PEG) bis(amine) (referred as MNPs) are attached with GdTx using a disuccinimidyl suberate (DSS) linker to obtain the conjugate of GdTx and MNPs (GdTx MNPs).

Figure 1 b shows transmission electron microscopy (TEM) images of core MNPs and GdTx MNPs. In accord with what is expected for a magnetic nanoparticle containing appended GdTx moieties, an MRI phantom study shows both T1 and T2 contrast enhancements.[11] Simultaneous T1 bright and T2 dark contrast are ascribable to the GdTx and MNPs portions

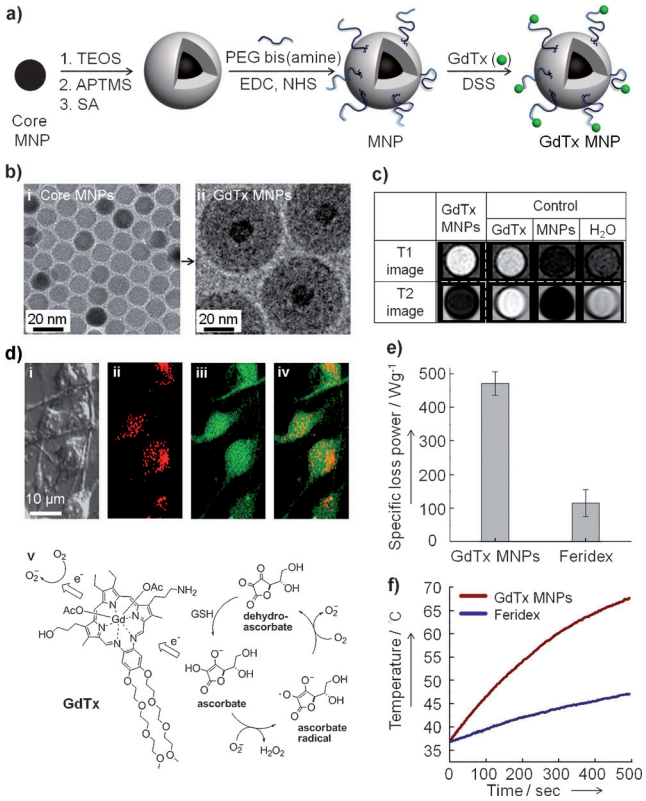

Figure 1. Synthesis of double effector nanoparticles (GdTx MNPs) and their features. a) Synthesis of GdTx MNPs. Magnetic nanoparticles are coated with SiO_2 and then amine-functionalized to conjugate with GdTx using DSS as a cross linker. b) TEM images of i) core MNPs and ii) GdTx MNPs. c) T1 and T2 MR phantom images of GdTx MNPs, GdTx, and MNPs. d) Intracellular uptake of GdTx MNPs and their ROS generation in MDA-MB-231 cells. Confocal microscopic images of MDA-MB-231 cells treated with GdTx MNPs. i) Differential interference contrast (DIC) image of GdTx MNP-treated MDA-MB-231 cells; ii) internalized GdTx MNPs visualized by the red fluorescence of GdTx; iii) ROS generation manifested by green fluorescence, which results from oxidation of 2′,7′-dichlorofluorescein diacetate (DCFA) to 2′,7′-dichlorofluorescein (DCF); iv) overlay of red and green fluorescence to give a yellow color; v) ROS generation by GdTx. e) Specific loss power (SLP) value of GdTx MNPs in comparison with that of Feridex in a 500 kHz AC magnetic field at 37.4 $kA\,m^{-1}$. f) Heat profile of 0.2 $mg\,mL^{-1}$ of GdTx MNPs and Feridex under an AC magnetic field for 500 seconds. APTMS = 3-aminopropyltrimethoxysilane, DSS = disuccinimidyl suberate, EDC = 1-ethyl-3-(3-dimethylaminopropyl)carbodiimide, GdTx = gadolinium texaphyrin, MNPs = magnetic nanoparticles, NHS = *N*-hydroxysuccinimide, PEG = polyethylene glycol, SA = succinic anhydride, TEM = transmission electron microscopy, TEOS = tetraethoxysilane.

of the constructs, respectively (Figure 1c). In contrast, MR images associated with the control groups display either only bright contrast for GdTx or dark contrast for MNPs, but not both.

The internalization of GdTx MNPs into cancer cells and the generation of ROS were examined using optical methods (Figure 1d). After the addition of GdTx MNPs to MDA-MB-231 cells, a weak red fluorescence signal is observed, which is ascribed to the GdTx portion of the internalized GdTx MNPs (Figure 1d(ii)). In analogy to what proved true for MGd, the internalized GdTx MNPs are expected to react with cellular metabolites, such as the ascorbate present in cancer cells, to generate ROS. The initial product of these electron-transfer processes is superoxide, which is eventually transformed to hydrogen peroxide (Figure 1d(v)). In the present case, ROS generation is clearly confirmed by a green fluorescence that has spread within the cells (Figure 1d(iii)). GdTx MNPs and ROS generation in the same cell are represented by the overlay of red and green fluorescence, resulting in a yellow color (Figure 1d(iv)).

GdTx MNPs display a high specific loss power (SLP) value (471 $W\,g^{-1}$), which is four times higher than the commercially available iron oxide nanoparticle, Feridex (Figure 1e). As a consequence, it only takes about 60 seconds to warm aqueous media from 37 °C to 43 °C with 0.2 $mg\,mL^{-1}$ of MNPs, whereas about 250 seconds are required to generate the same degree of warming using an equivalent amount of Feridex under otherwise identical conditions (Figure 1f). The reduced amount of GdTx MNPs for adequate heat generation is considered a useful feature that may permit lower dosage levels when translated into a clinical setting.

The utility of the dual-effector nature of the GdTx MNPs (ROS and heat) were first tested in vitro. Towards this end, MDA-MB-231 cells (1.0×10^4 cells/well) and 0.2 $mg\,mL^{-1}$ of GdTx MNPs were co-incubated for 5 h under conditions where the concentration of the GdTx is 100 μM. An AC magnetic field was then applied (Figure 2a). The temperature of the medium was increased to 43 ± 1 °C and then maintained for up to 60 min (Figure 2b). Cell viability was then measured by CCK-8 assay. In the case of the bare MNPs, cell viability decreased monotonically from 100% to 98%, 90%, 83%, and 75% (blue line, Figure 2c) as the time of the hyperthermia treatment was increased (i.e., 0, 10, 20, 30, and 60 min). In contrast, GdTx MNPs significantly reduce the cell viability from 93% to 76%, 66%, 42%, and 36% as the treatment time increases (0, 10, 20, 30, and 60 min; red line, Figure 2c).

The slight loss in cell viability observed before magnetic hyperthermia is initiated ($t = 0$; red line, Figure 2c) is caused by surface-coated GdTx, an agent that is known for its weak but noticeable anticancer effect through ROS generation.[12] Although ROS itself show little anticancer effect, ROS production dysregulates cancer cell redox homeostasis and induces oxidative stress. In turn, these effects are expected to render the cells more susceptible to magnetic heat treatment. In the present case, the production of ROS is likely to give rise to a synergistic effect in combination with hyperthermia.

In terms of experiment, the synergistic dual effect is the most significant at 30 min of thermal treatment, where 57% of the cancer cells are eliminated by the GdTx MNPs after an AC magnetic field application, whereas only 17% of cancer cells are nonviable with MNPs.

As the relative GdTx loading level on the MNPs was increased from 0 to 1500 and 3000 (that is, the number of GdTx molecules conjugated to a given MNP), the cell death markedly increased from 17% to 21%, and 57% under magnetic hyperthermia conditions (red line, Figure 2d). In contrast, the number of nonviable cells increased only from 0% to 3% and then 7% as the loading level was raised in the

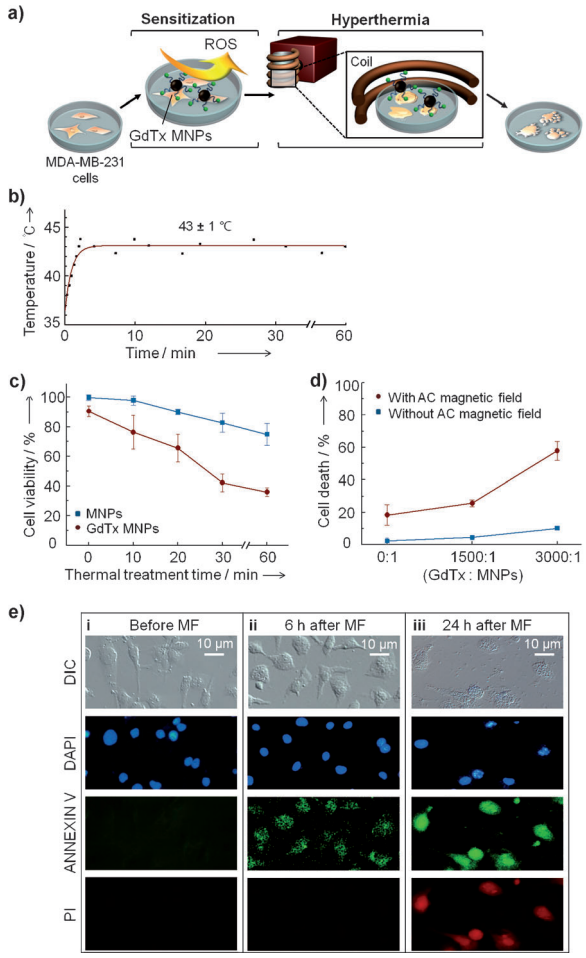

Figure 2. In vitro magnetic hyperthermia studies involving the GdTx MNPs and MDA-MB-231 cells. a) Illustration of the in vitro experiment. Briefly, GdTx MNP-treated MDA-MB-231 cells are incubated for 5 h and then an AC magnetic field is applied to effect hyperthermia. b) Temperature profile. A temperature of 43 ± 1 °C is maintained in an AC magnetic field of 37.4 kA m^{-1} at 500 kHz. c) Time dependence of the magnetic hyperthermia treatment effect. d) Dependence of the magnetic hyperthermia efficacy on GdTx loading level. e) Monitoring of MDA-MB-231 cell death pathway induced by magnetic hyperthermia using GdTx MNPs. Microscopic images of MDA-MB-231 cells before (i), and 6 h (ii) and 24 h (iii) after magnetic field (MF) application. In these experiments, the nuclei are stained with DAPI (4′,6-diamidino-2-phenylindole; blue), and membrane inversion followed by membrane rupture is detected by annexin V-FITC (annexin V–fluorescein isothiocyanate; green) and propidium iodide (red, PI).

absence of an applied AC magnetic field (blue line, Figure 2d). This result indicates that the dominant role of GdTx is as a sensitizer for hyperthermia rather than as direct cytotoxin.

GdTx MNP-mediated hyperthermia can kill cancer cells by a number of pathways,[13] including apoptosis and necrosis. To determine the predominant cell death pathway induced by the GdTx MNPs, standard annexin V–fluorescein isothiocyanate (annexin V–FITC) and propidium iodide (PI) staining studies were carried out (Figure 2e). These assays detect changes in plasma membrane integrity and the release of DNA. Apoptosis initially induced the inversion of phosphatidylserine, which allows binding to annexin V–FITC, while PI is unable to enter into the cells to bind DNA at this initial stage. Before AC magnetic field application, neither annexin V–FITC nor PI-stained cells are detected (Figure 2e(i)). At 6 h post-hyperthermia treatment, only annexin V–FITC stained cells are detected, indicating that the cause of cell death is primarily apoptosis (Figure 2e(ii)). If necrosis were occurring, a red fluorescence would be observed early on as the result of PI–DNA interactions following membrane rupture. At 24 h post-hyperthermia treatment, both annexin V–FITC and PI-stained cells are observed, which is due to membrane rupture, a classic hallmark of late-stage apoptosis (Figure 2e(iii)). These results are thus fully consistent with the notion that GdTx MNP hyperthermia occurs predominantly through apoptosis.

We further tested the efficacy of GdTx MNP-induced magnetic hyperthermia in vivo. MDA-MB-231 breast cancer cells were xenografted to the right hind leg of nude mice in several experimental groups ($n = 3$). GdTx MNPs (75 μg), dispersed in normal saline (50 μL), were directly injected into the tumor (100 mm^3). Then, the mouse was placed in a water-cooled magnetic induction coil (Figure 3a) and AC magnetic field (500 kHz at 37.4 kA m^{-1}) was applied to maintain a constant temperature at the tumor (43 ± 1 °C) for 30 min. After a single hyperthermia treatment, the tumor size was monitored for 14 days. In the mice making up the untreated control group, the tumor size had increased approximately sevenfold by day 14 (Figure 3b,c). However, for the group

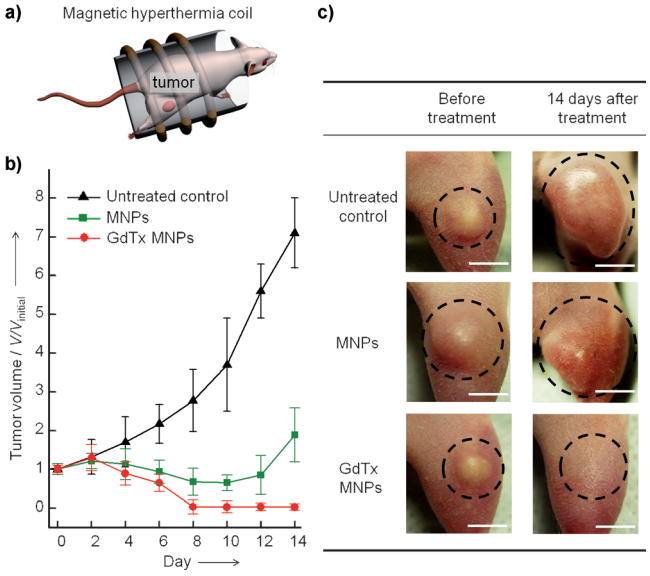

Figure 3. In vivo magnetic hyperthermia. a) Representation of the in vivo magnetic hyperthermia study. Magnetic nanoparticles (75 μg) are directly injected into the tumor (tumor volume 100 mm^3, $n = 3$) of a mouse and subjected to an AC field for 30 min at 43 ± 1 °C. b) Plot of tumor volume ($V/V_{initial}$) versus the number of days after treatment. In the group treated with GdTx MNP hyperthermia (red line), the tumor is completely eliminated by day 8, whereas the MNP hyperthermia group (green line) shows only initial reduction in tumor volume, followed by regrowth. c) Images of xenografted tumors (MDA-MB-231) on nude mice before treatment (left column) and 14 days after treatment (right column). Scale bars: 5 mm.

receiving hyperthermia treatment with GdTx MNPs, the tumor was clearly eliminated within 8 days (Figure 3b,c). For comparison, another group of mice was subjected to hyperthermia treatment after administration of bare MNPs at an identical dosage. Although the size of tumor regresses initially, a significant amount of tumor remained at day 8 ($V/V_{initial} = 0.6$) and the tumor started to regrow at day 12.

This study, based on the use of double-effector nanoparticles, has demonstrated a new approach to achieving apoptotic magnetic hyperthermia. Until now, attempts of magnetic hyperthermia at low temperature have been challenging owing to the development of thermotolerance. The dramatic reduction in tumor burden seen in vivo and the high degree of efficacy seen in vitro are ascribed to the sensitization effect arising from ROS, which clearly play a key role in enhancing the treatment efficacy. Efficient heat generation by GdTx MNPs for targeting low temperature (43 °C) is also advantageous because lower concentrations of nanoparticles are required to achieve the same biological effect. The pathway of cell death predominantly involves apoptosis, a mode of action that is considered beneficial for ultimate clinical use. Prior to the present study, low-temperature hyperthermia and high therapeutic efficacy have been incompatible. However, the use of the present double-effector nanoparticle system allows these seemingly disparate goals to be realized. More broadly, we have shown that it is possible to achieve efficient apoptotic hyperthermia at low temperature.

Received: August 9, 2012
Published online: November 8, 2012

Keywords: apoptosis · gadolinium texaphyrin · hyperthermia · magnetic nanoparticles · reactive oxygen species

[1] M. J. Kluger, *Fever: Its Biology, Evolution, and Function*, Princeton University Press, Princeton, **1979**.

[2] a) Y. Su, X. Wei, F. Peng, Y. Zhong, Y. Lu, S. Su, T. Xu, S.-T. Lee, Y. He, *Nano Lett.* **2012**, *12*, 1845 – 1850; b) J. A. Barreto, W. O'Malley, M. Kubeil, B. Graham, H. Stephan, L. Spiccia, *Adv. Mater.* **2011**, *23*, H18 – H40; c) W.-S. Kuo, C.-N. Chang, Y.-T. Chang, M.-H. Yang, Y.-H. Chien, S.-J. Chen, C.-S. Yeh, *Angew. Chem.* **2010**, *122*, 2771 – 2775; *Angew. Chem. Int. Ed.* **2010**, *49*, 2711 – 2715; d) K.-W. Hu, T.-M. Liu, K.-Y. Chung, K.-S. Huang, C.-T. Hsieh, C.-K. Sun, C.-S. Yeh, *J. Am. Chem. Soc.* **2009**, *131*, 14186 – 14187; e) J.-P. Fortin, C. Wilhelm, J. Servais, C. Ménager, J.-C. Bacri, F. Gazeau, *J. Am. Chem. Soc.* **2007**, *129*, 2628 – 2635; f) M. Hiraoka, Y. Nagata, M. Mitsumori, M. Sakamoto, S. Masunaga, *AIP Conf. Proc.* **2004**, *716*, 102 – 105.

[3] a) M. Colombo, S. Carregal-Romero, M. F. Casula, L. Gutiérrez, M. P. Morales, I. B. Böhm, J. T. Heverhagen, D. Prosperi, W. J. Parak, *Chem. Soc. Rev.* **2012**, *41*, 4306 – 4334; b) S.-h. Noh, W. Na, J.-t. Jang, J.-H. Lee, E. J. Lee, S. H. Moon, Y. Lim, J.-S. Shin, J. Cheon, *Nano Lett.* **2012**, *12*, 3716 – 3721; c) K. H. Bae, M. Park, M. J. Do, N. Lee, J. H. Ryu, G. W. Kim, C. Kim, T. G. Park, T. Hyeon, *ACS Nano* **2012**, *6*, 5266 – 5273; d) P. Guardia, R. Di Corato, L. Lartigue, C. Wilhelm, A. Espinosa, M. Garcia-Hernandez, F. Gazeau, L. Manna, T. Pellegrino, *ACS Nano* **2012**, *6*, 3080 – 3091; e) L. Lartigue, C. Innocenti, T. Kalaivani, A. Awwad, M. del Mar Sanchez Duque, Y. Guari, J. Larionova, C. Guerin, J.-L. G. Montero, V. Barragan-Montero, P. Arosio, A. Lascialfari, D. Gatteschi, C. Sangregorio, *J. Am. Chem. Soc.* **2011**, *133*, 10459 – 10472; f) J.-H. Lee, J.-t. Jang, J.-s. Choi, S. H. Moon, S.-h. Noh, J.-w. Kim, J.-G. Kim, I.-S. Kim, K. I. Park, J. Cheon, *Nat. Nanotechnol.* **2011**, *6*, 418 – 422; g) D. Ho, X.-L. Sun, S.-H. Sun, *Acc. Chem. Res.* **2011**, *44*, 875 – 882; h) D. Yoo, J.-H. Lee, T.-H. Shin, J. Cheon, *Acc. Chem. Res.* **2011**, *44*, 863 – 874; i) A. J. Cole, V. C. Yang, A. E. David, *Trends Biotechnol.* **2011**, *29*, 323 – 332; j) K. Riehemann, S. W. Schneider, T. A. Luger, B. Godin, M. Ferrari, H. Fuchs, *Angew. Chem.* **2009**, *121*, 886 – 913; *Angew. Chem. Int. Ed.* **2009**, *48*, 872 – 897; k) D. Shi, H. S. Cho, Y. Chen, H. Xu, H. Gu, J. Lian, W. Wang, G. Liu, C. Huth, L. Wang, R. C. Ewing, S. Budko, G. M. Pauletti, Z. Dong, *Adv. Mater.* **2009**, *21*, 2170 – 2173; l) F. Sonvico, S. Mornet, S. Vasseur, C. Dubernet, D. Jaillard, J. Degrouard, J. Hoebeke, E. Duguet, P. Colombo, P. Couvreur, *Bioconjugate Chem.* **2005**, *16*, 1181 – 1188.

[4] a) K. L. O'Neill, D. W. Fairbairn, M. J. Smith, B. S. Poe, *Apoptosis* **1998**, *3*, 369 – 375; b) B. V. Harmon, A. M. Corder, R. J. Collins, G. C. Gobé, J. Allen, D. J. Allan, J. F. R. Kerr, *Int. J. Radiat. Biol.* **1990**, *58*, 845 – 858.

[5] D. Kanduc, A. Mittelman, R. Serpico, E. Sinigaglia, A. A. Sinha, C. Natale, R. Santacroce, M. G. Di Corcia, A. Lucchese, L. Dini, P. Pani, S. Santacrose, S. Simone, R. Bucci, E. Farber, *Int. J. Oncol.* **2002**, *21*, 165 – 170.

[6] a) P. Golstein, G. Kroemer, *Trends Biochem. Sci.* **2007**, *32*, 37 – 43; b) R. D. Bonfil, O. D. Bustuoabad, R. A. Ruggiero, R. P. Meiss, C. D. Pasqualini, *Clin. Exp. Metastasis* **1988**, *6*, 121 – 129.

[7] a) J. T. Beckham, G. J. Wilmink, S. R. Opalenik, M. A. Mackanos, A. A. Abraham, K. Takahashi, C. H. Contag, T. Takahashi, E. D. Jansen, *Lasers Surg. Med.* **2010**, *42*, 752 – 765; b) L. Huang, N. F. Mivechi, D. Moskophidis, *Mol. Cell. Biol.* **2001**, *21*, 8575 – 8591; c) E. A. A. Nollen, J. F. Brunsting, H. Roelofsen, L. A. Weber, H. H. Kampinga, *Mol. Cell. Biol.* **1999**, *19*, 2069 – 2079.

[8] a) J. van der Zee, *Ann. Oncol.* **2002**, *13*, 1173 – 1184; b) L. F. Fajardo, *Cancer Res.* **1984**, *44*, 4826 – 4835; c) National Cancer Institute (2011) *Hyperthermia in Cancer Treatment.* Available at: http://www.cancer.gov/cancertopics/factsheet/Therapy/hyperthermia (accessed Aug 7, 2012).

[9] a) D. Magda, R. A. Miller, *Semin. Cancer Biol.* **2006**, *16*, 466 – 476; b) D. Magda, C. Lepp, N. Gerasimchuk, I. Lee, J. L. Sessler, A. Lin, J. Biaglow, R. A. Miller, *Int. J. Radiat. Oncol. Biol. Phys.* **2001**, *51*, 1025 – 1036; c) D. Magda, C. Lepp, N. Gerasimchuk, P. Lecane, R. A. Miller, J. E. Biaglow, J. L. Sessler, *Chem. Commun.* **2002**, 2730 – 2731.

[10] J.-t. Jang, H. Nah, J.-H. Lee, S. H. Moon, M. G. Kim, J. Cheon, *Angew. Chem.* **2009**, *121*, 1260 – 1264; *Angew. Chem. Int. Ed.* **2009**, *48*, 1234 – 1238.

[11] J.-s. Choi, J.-H. Lee, T.-H. Shin, H.-T. Song, E. Y. Kim, J. Cheon, *J. Am. Chem. Soc.* **2010**, *132*, 11015 – 11017.

[12] G. T. Wondrak, *Antioxid. Redox Signaling* **2009**, *11*, 3013 – 3069.

[13] a) H. Okada, T. W. Mak, *Nat. Rev. Cancer* **2004**, *4*, 592 – 603; b) J. Marx, *Science* **1993**, *259*, 760 – 761; c) G. T. Williams, *Cell* **1991**, *65*, 1097 – 1098.

